Practical applications of the multi-component marine photosynthesis model (MCM)*

OCEANOLOGIA, 45 (3), 2003.
pp. 395–423.

KEYWORDS
Bio-optical modelling
Quantum yield
of photosynthesis
Primary production
Inorganic nitrogen
Tropical zone
Temperate zone
Polar zone

Dariusz Ficek[2]
Roman Majchrowski[2]
Mirosława Ostrowska[1]
Sławomir Kaczmarek[1]
Bogdan Woźniak[1]
Jerzy Dera[1]

[1] Institute of Oceanology,
Polish Academy of Sciences,
Powstańców Warszawy 55, PL–81–712 Sopot, Poland

[2] Institute of Physics,
Pomeranian Pedagogical Academy in Słupsk,
Arciszewskiego 22 B, PL–76–200 Słupsk, Poland;

e-mail: darek@wsp.slupsk.pl

Manuscript received 18 July 2003, reviewed 5 August 2003, accepted 19 August 2003.

Abstract

This paper describes the applications and accuracy analyses of our multi-component model of marine photosynthesis, given in detail in Woźniak et al. (2003). We now describe an application of the model to determine quantities characterising the photosynthesis of marine algae, especially the quantum yield of photosynthesis

* This work was carried out within the framework of IO PAN's statutory research, and also as part of project PZB–KBN 056/PO4/2001/3 of the Institute of Physics, Pomeranian Pedagogical Academy in Słupsk.

and photosynthetic primary production. These calculations have permitted the analysis of the variability of these photosynthesis characteristics in a diversity of seas, at different seasons, and at different depths.

Because of its structure, the model can be used as the 'marine part' of a 'satellite' algorithm for monitoring primary production in the sea (the set of input data necessary for the calculations can be determined with remote sensing methods). With this in mind, in the present work, we have tested and verified the model using empirical data. The verification yielded satisfactory results: for example, the statistical errors in estimates of primary production in the water column for Case 1 Waters do not exceed 45%. Hence, this model is far more accurate than earlier, less complex models hitherto applied in satellite algorithms.

1. Introduction

The following six detailed groups of models were presented in the paper by Woźniak et al. (2003):

(1) statistical models of vertical chlorophyll distributions $C_a(z)$ in the sea derived for stratified seas (after Woźniak et al. 1992a, b) and Baltic basins containing well-mixed water masses (after Woźniak et al. 1995b);

(2) bio-optical underwater irradiance transmittance models for oceanic Case 1 Waters (after Woźniak et al. 1992a, b) and for Baltic Case 2 Waters (after Kaczmarek & Woźniak 1995);

(3) a statistical model of the photo- and chromatic acclimation of phytoplankton, which contains model formulas enabling the concentrations of particular photosynthetic and photoprotecting pigments to be determined (after Majchrowski & Ostrowska 1999, 2000, Majchrowski 2001);

(4) a model of light absorption by phytoplankton *in vivo* (after Woźniak et al. 1999, 2000, Majchrowski et al. 2000) that takes account of the photo– and chromatic adaptation effects and the packaging effect of pigments in the cell;

(5) statistically generalised relationships within a set of given environmental parameters: inorganic nitrogen concentrations vs chlorophyll *a* concentrations *vs* temperature in the sea, permitting in particular the estimation from satellite data of nitrogen concentrations at different depths in the sea (after Ficek 2001);

(6) a model of the quantum yield of marine photosynthesis enabling this yield to be determined at different depths on the basis of such environmental factors as irradiance conditions, nitrogenous nutrient content, water temperature, and basin trophicity (after Ficek et al. 2000a, b, Woźniak & Dera 2000, 2001, Woźniak et al. 2002a, b).

These models describe a broad set of processes involving the inflow, absorption and utilisation of light energy in marine ecosystems under a variety of environmental conditions. Furthermore, an appropriately detailed synthesis of these models has been applied to construct a general, multi-component model of photosynthesis in the sea (see the block diagram of Fig. 1 in Woźniak et al. (2003) – also available on the Internet at www.iopan.gda.pl/oceanologia). To simplify further description, this multi-component model, together with the relevant algorithm published in the same paper (Woźniak et al. 2003), will here be denoted by the abbreviation MCM. With this model, diverse optical and bio-optical characteristics of sea water and the photosynthetic properties of phytoplankton can be approximately estimated from three input data: (i) the concentration of chlorophyll $C_a(0)$ in the sea surface layer, i.e. a trophicity index of the basin, (ii) the irradiance conditions at the sea surface, represented, for instance, by the solar irradiance crossing the air-sea interface in the photosynthetically available spectral range $PAR(0^+)$, and (iii) the temperature of the sea surface water $temp(0)$. In a more accurate version of the model the nutrient content (nitrogen) is used as a fourth input data. The complete mathematical apparatus of the MCM is given in a condensed and practically useful form in Annex 1 of the paper by Woźniak et al. (2003). It permits the analysis of, among other things, the range of variability of the photosynthesis quantum yield and natural primary production of organic matter in different seas, at different seasons and in different parts of the world ocean, not to mention different depths in the water. This analysis is presented in the previous paper by Woźniak et al. (2003).

The two main aims of the present paper are: (1) to apply the model relationships in the determination of the main characteristics of photosynthesis – the quantum yield and primary production – in different seasons, regions and depths of the world ocean on the basis of known irradiance conditions, nutrient content, temperature and basin trophicity, and (2) to estimate the errors of these calculations and compare the accuracy of the MCM with previous, less complex models of a similar nature applied in remote sensing algorithms.

In this respect a model calculation has been done and its results are presented in section 2. Furthermore, a validation of the MCM, as the marine part of the satellite algorithm, based on the three fundamental input variables only and also on the nutrient content calculation, has been performed and is given in section 3. For comparison, validations of primary production estimates on the same empirical material were carried out using two simpler models of the quantum yield of photosynthesis in the sea, one developed earlier by our team (Woźniak et al. 1992a, b, 1995b, Dera 1995),

summarised in Annex 1, the other by our French colleagues (Morel 1991, Antoine & Morel 1996, Morel et al. 1996), summarised in Annex 2.

2. Application of the modelling to estimate the photosynthetic quantum yield and primary production at different seasons and in the Earth's various marine systems

2.1. The range of calculations

In order to characterise the variation in the naturally occurring range of variability of the quantum yield of photosynthesis Φ and primary production P in the sea, the vertical profiles of this yield $\Phi(z)$ and the production $P(z)$ were modelled for different climatic zones, diverse optical-dynamic-climatic types of seas and their associated trophic types of waters, and also for two seasons – June (the northern summer) and December (the northern winter). Three climatic zones were distinguished: a tropical zone (0–10°N), a temperate zone (∼40°N) and a polar zone (∼60°N). Apart from the depth in the sea, the fundamental variables in the model, the input data for the computations (see Table 1) were:

- the surface concentration of chlorophyll $C_a(0)$;
- the solar (scalar) irradiance within the spectral range 400–700 nm penetrating beneath the sea surface $PAR_0(0^+)$;
- the temperature of the surface water layer *temp*, which, to simplify matters, was taken to be representative of and constant at all depths in layers with significant primary production.

The surface irradiance within the spectral range 400–700 nm, $PAR_0(0^+)$, was estimated from the monthly mean total daily doses of solar irradiance at the sea surface $<\eta_{\mathrm{day}}>_{\mathrm{month}}$, typical of these geographical regions and months, given in Timofeyev's monograph (1983). The instantaneous values of this irradiance were determined from the duration of daylight and by simulating the sinusoidal sequences of this irradiance during the day.

The relevant seawater temperatures were taken from the temperature data of seas and oceans at different seasons and in different regions given in the monograph by Gershanovich & Muromtsev (1982).

On the other hand, the surface chlorophyll concentrations $C_a(0)$ serving as input data were the relevant sets of indices of the various trophic types of sea. Only those trophic and optical-dynamic-climatic types were chosen that could occur in a given geographical area and season, the selection being made on the basis of the temperatures given in Fig. 11 of the MCM description – available on the Internet at www.iopan.gda.pl/oceanologia.

Table 1. Input data of the modelling

- $<\eta_{\mathrm{day}}>_{\mathrm{month}}$ – monthly mean total daily doses of solar irradiance at the sea surface in various geographic regions of the world ocean (after Timofeyev 1983);
- *temp* – temperature of the sea (after Gershanovich & Muromtsev 1982);
- chlorophyll concentrations (are given for the various types of seas in Annex 3, Table A 3.1)

Geographical zone	Season of the year						Range of calculation		
	Summer (June)			Winter (January)				trophic type of sea**	
	temperature *temp* [°C]	$<\eta_{\mathrm{day}}>_{\mathrm{month}}$ [MJ m^{-2} day^{-1}]	duration of daylight t_d [h]	temperature *temp* [°C]	$<\eta_{\mathrm{day}}>_{\mathrm{month}}$ [MJ m^{-2} day^{-1}]	duration of daylight t_d [h]	optical-dynamic-climatic types of the sea*	summer	winter
1	2	3	4	5	6	7	8	9	10
tropical (0–10°N)	27	19.6	12	25	18.6	12	Case 1 (S–W) Case 2 (M–W)	O1–I I	O1–I I
temperature (40°N)	20	21.4	14.8	10	8	9.5	Case 1 (S–W) Case 2 (M–W)	O1–I I	O1–E2 E1–E2
polar (60°N)	5	13.5	18.4	1	0.4	6.3	Case 1 (S–C) Case 2 (M–C)	O1–E3 E2–E3	O1–E2 I–E1

* Case 1, Case 2 – optical water types according to Morel & Prieur (1977); (S–W) – stratified, warm (i.e. temperature > 6°C); (M–W) – mixed, warm; (S–C) – stratified cold (i.e. temperature ≤ 6°C); (M–C) – mixed, cold; according to Woźniak et al. (2003 – the MCM description).

** with various chlorophyll concentrations as given in Annex 3, Table A3.1.

Surface chlorophyll concentrations $C_a(0)$ and temperature *temp* were also used to estimate the corresponding nitrogen concentrations $N_{\mathrm{inorg}}(0)$ (eq. (A1.31) in the MCM description), from which, in turn, the complete vertical distributions of nitrogenous nutrients $N_{\mathrm{inorg}}(z)$ could be found (eq. (A1.32) and (A1.33) in the MCM description). In all calculations of $N_{\mathrm{inorg}}(z)$ from $N_{\mathrm{inorg}}(0)$ the mixing depth was assumed to be $z_m = 50\,\mathrm{m}$. The plots of the vertical distributions of inorganic nitrogen determined in this way for all the model calculations are shown on the graphs marked with the letter a on Figs. 1–3.

2.2. Results of the calculation and its discussion

The magnitudes of the quantum yield of photosynthesis of algae $\Phi(z)$ and their primary production $P(z)$ at different depths in different marine systems, and of the total production in the water column P_{tot} were computed with the aid of the algorithm given in Annex 1 of the MCM description. The input data used in these calculations were discussed earlier in this paper. The depth profiles of the quantum yield of photosynthesis averaged over the whole day, and the daily productions in different types of sea in different seasons and geographical areas are shown in Figs. 1–3 (the relevant plots are denoted by the letters b and c). Also the total 24-hour primary productions P_{tot} (i.e. in the water column beneath unit area) for all cases are given in Table 2.

The results show up a number of distinct regularities that are independent of climatic zone. First, the yield $\Phi(z)$ generally rises with the surface concentration of chlorophyll $C_a(0)$ and its associated trophic type; the highest yields occur in eutrophic waters.

The next regularity concerns the depth at which maximum yields occur: their positions vary with trophic type. The depths are greatest in oligotrophic seas and, as the productivity class of the water increases, these depths become shallower. Above and below these maxima the yield decreases: the low values at the surface are the consequence of intense irradiance; on the other hand, at large depths the yield drops to around $0.05\ \mathrm{mol\,C\ Ein^{-1}}$, this fall being due to the decline in the number of active reaction centres.

The results of modelling absolute magnitudes of primary production at different depths $P(z)$ and the total production in the water column P_{tot} (Table 2) also demonstrate the existence of certain regularities regardless of climatic zone. Often already well-known from empirical studies, here they are reiterated quantitatively in more precise terms.

Thus, in all cases, the production $P(z)$ varies very considerably with depth. The distributions of the vertical profiles of $P(z)$ are usually

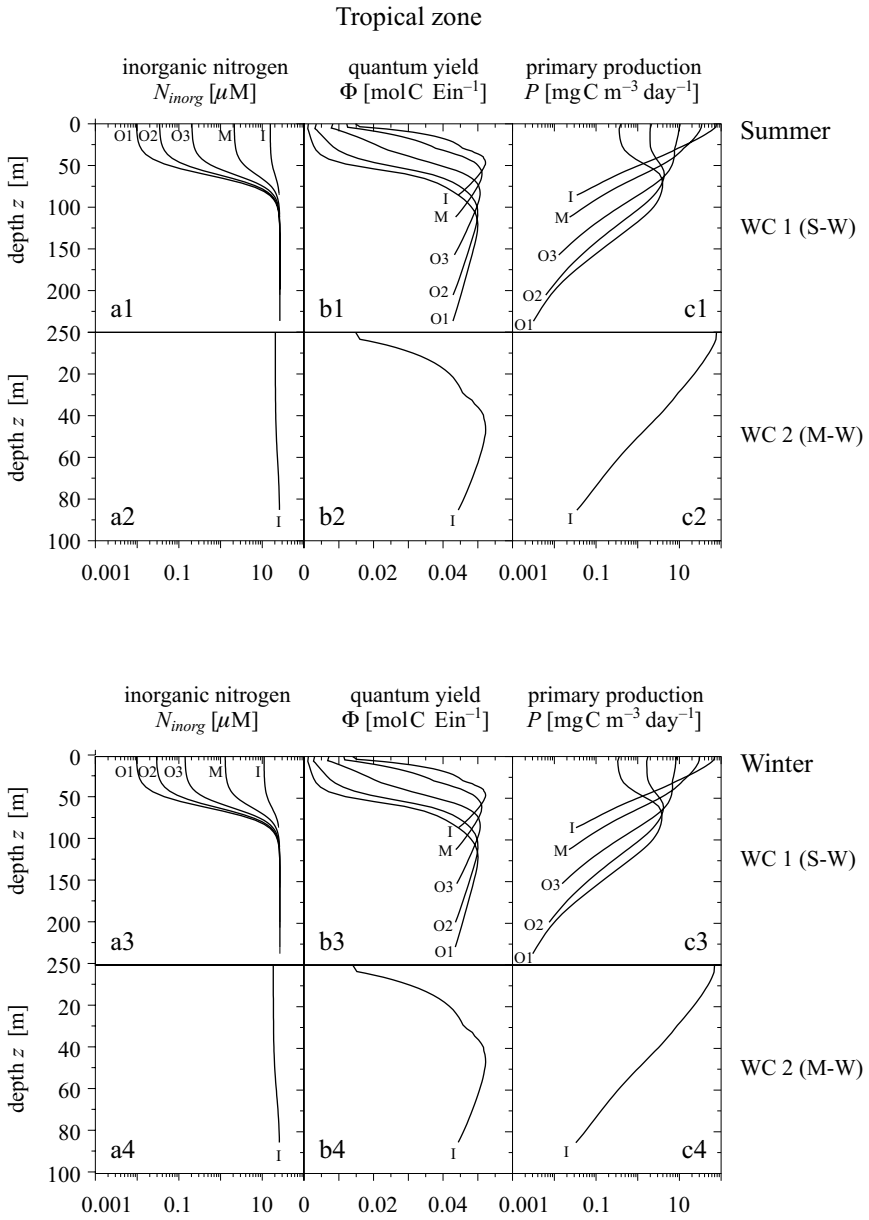

Fig. 1. Modelled vertical profiles: concentration of inorganic nitrogen (a), quantum yield of photosynthesis (b) and primary production (c) in tropical seas (explanation in the text)

monomodal, that is, they display a single, main peak. Below this maximum, production falls rapidly with depth; it is, as we know, practically directly proportional to the level of PAR irradiance. However, in the layers above the

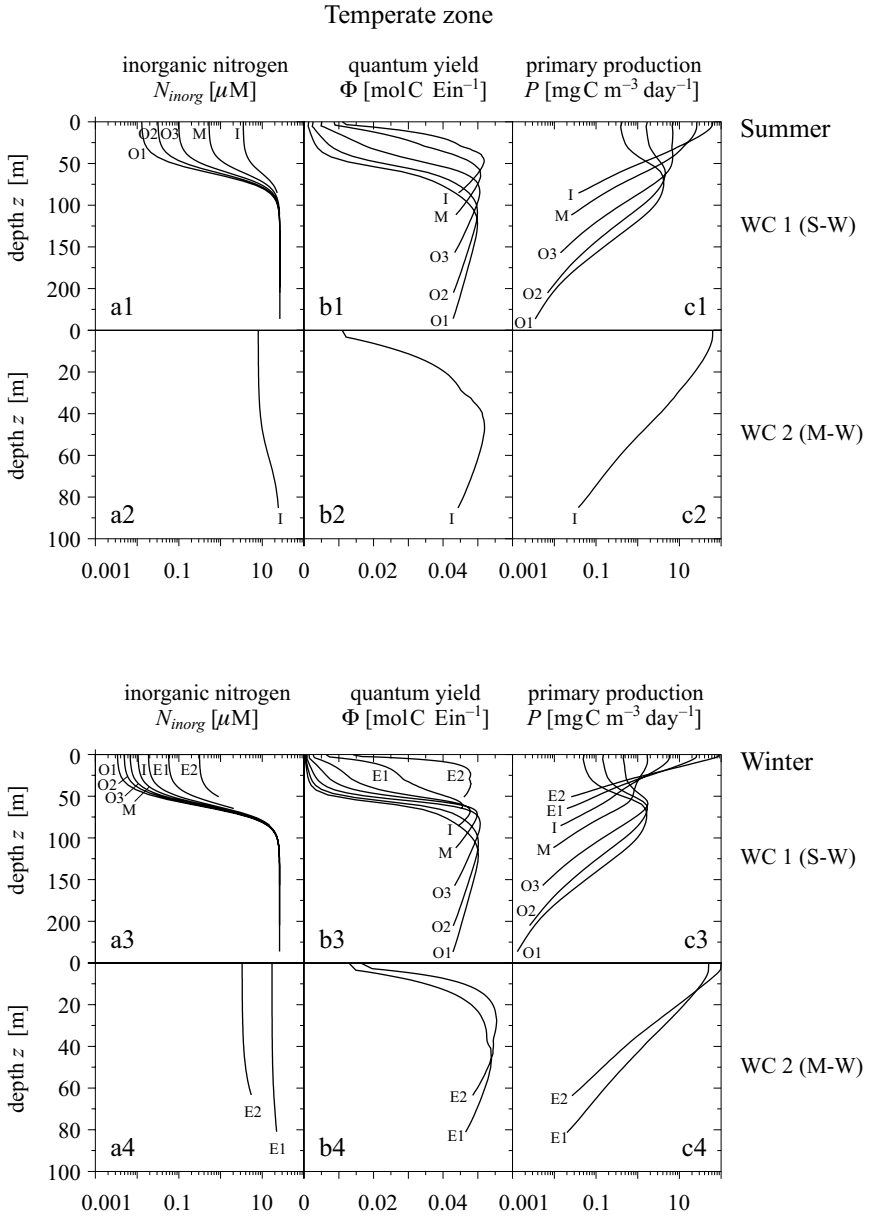

Fig. 2. Modelled vertical profiles: concentration of the inorganic nitrogen (a), quantum yield of photosynthesis (b), and primary production (c) in temperate seas (explanation in the text)

maximum, the fall-off in production may be equally abrupt, but then again, it may not occur at all. The distinctness of this maximum and its position depend on the trophic type of the sea. It is the most distinct and occurs

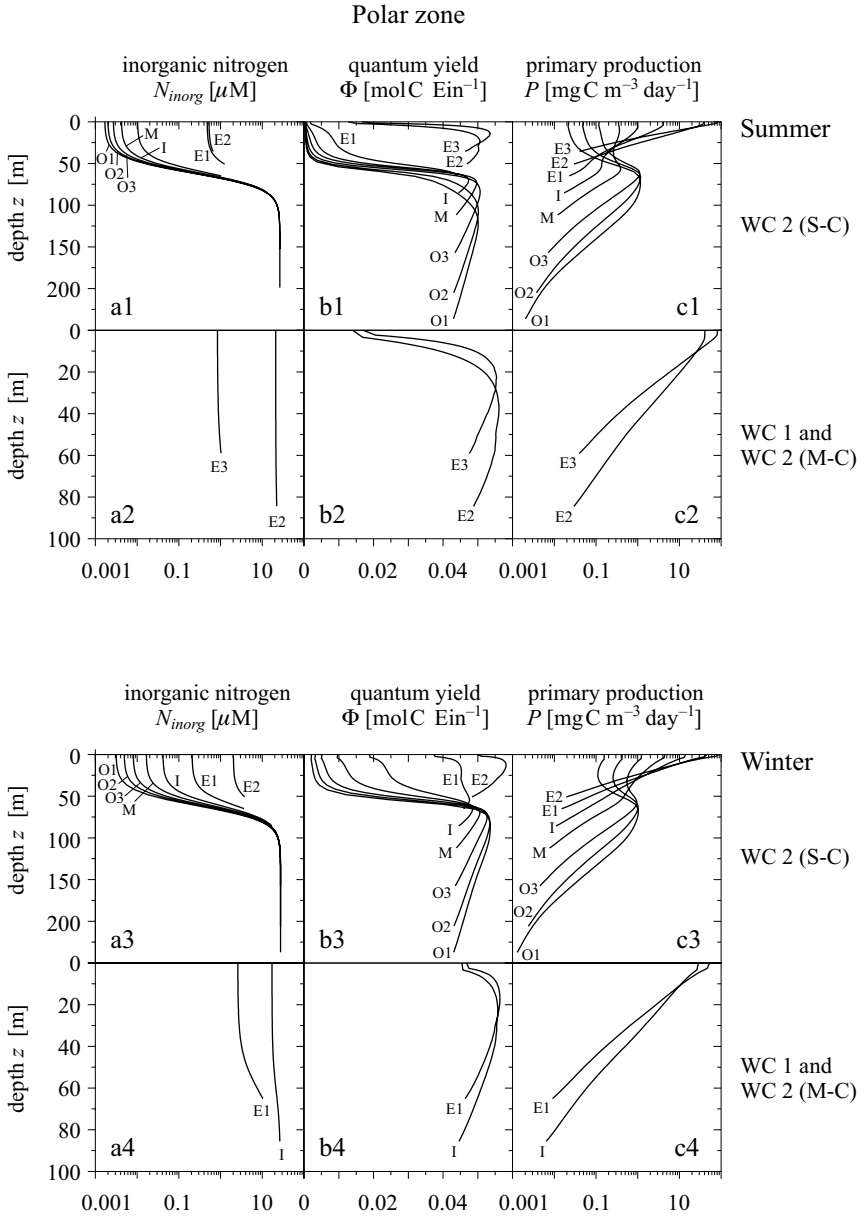

Fig. 3. Modelled vertical profiles: concentration of inorganic nitrogen (a), quantum yield of photosynthesis (b), and primary production (c) in polar seas (explanation in the text)

at the greatest depths in oligotrophic waters. For instance, in O1 and O2 type seas, production is greatest at around 60–90 metres, where it exceeds the typical values for surface layers by at least one order of magnitude. As

Table 2. Daily primary production P_{tot} [mg C m^{-2}] determined from the MCM for various types of sea in different geographical regions and different seasons; the values can be assumed to be typical

Region	Season	Type and trophicity											
		Case 1 (S–W)								Case 2 (M–W)			
		O1	O2	O3	M	I	E1	E2	E3	I	E1	E2	E3
tropical (0–10°N)	summer (June)	243	297	565	926	1262				1263			
	winter (January)	229	270	497	848	1167				1169			
temperature (40°N)	summer (June)	262	298	492	784	1190				1201			
	winter (January)	90	81	80	75	122	326	725			645	843	
		Case 1 (S–C)								Case 2 (M–C)			
		O1	O2	O3	M	I	E1	E2	E3	I	E1	E2	E3
polar (60°N)	summer (June)	140	115	90	48	59	155	1186	1627			1326	1688
	winter (January)	6	6	7	10	22	54	79		53	67		

the trophicity of a basin increases, however, starting with type O3, this tendency becomes much weaker. At the same time, the position of the maximum moves closer to the surface.

A second characteristic aspect of primary production in various parts of the World Ocean under all climatic regimes and at all times of the year is the relation between absolute values of production and the chlorophyll concentration, that is, with the trophicity of the waters. Production is, of course, greatest in eutrophic waters, where values are c. 5 and sometimes c. 15 times greater than in oligotrophic waters in the same climatic zones and the same seasons.

Regardless of these regularities involving the vertical distributions $\Phi(z)$, $P(z)$, there is a whole range of zonal regularities which are independent both of the geographical region where they occur and of the season of the year. This relates in particular to the absolute values of primary production $P(z)$ and P_{tot}. These will now be discussed.

Waters of the tropical zone

Example vertical profiles of the quantum yield of photosynthesis in the sea, $\Phi(z)$, for tropical waters in summer are shown in Fig. 1 (plots b1, b2, b3, b4). Fig. 1 b1 corresponds to a temperature of 27°C and refers to seas of the optical-dynamic-climatic type Case 1 (S–W). The figure shows five plots of $\Phi(z)$, since the ordinate for *temp* = 27°C in this region cuts the five $C_a(0)$ isolines indicative of the basin trophic types O1, O2, O3, M, I as given in Fig. 11 of the MCM description (see Woźniak et al. 2003). The largest yield at the sea surface is c. 0.015 mol C Ein^{-1} and is recorded in the intermediate basin trophic type I. As the surface concentration of chlorophyll falls, so does the yield, which drops to a minimum in oligotrophic waters. Analysis of the relation between yield and depth shows that the former gradually increases, and at a depth of about 1.1 z_e (i.e. at an optical depth of c. $\tau \approx 5$), the yield attains maximum values, which may be as high as 0.05 mol C Ein^{-1}. Type Case 2 (M–W) under the same conditions is represented by only one $\Phi(z)$ plot, which corresponds to basin trophic type I (see Fig. 1 b2).

The situation typically obtaining in tropical waters during winter is illustrated in Figs. 1 b3 and 1 b4, from which it is evident that yields $\Phi(z)$ take roughly the same values as in summer. This is due to the minimal seasonal changes in the environment: the temperature variation amplitude of ± 1°C, and the irradiance dose amplitude of c. ± 2.5%. The quantum yield of photosynthesis in tropical regions is thus practically constant, that is to say, independent of the time of year.

Plots c1, c2, c3, c4 in Fig. 1 show the vertical distributions of primary production for the same types of seas in the tropical zone. For the same reasons as in the case of the quantum yield of photosynthesis $\Phi(z)$, the absolute magnitudes of this production at different depths $P(z)$ and the total production P_{tot} (see upper part of Table 2) in tropical seas are also practically the same in summer and winter. A further point worth making is that these are the highest values of primary production for this particular trophic type of waters. In other climatic zones, these absolute values for the same trophic types of waters are lower, in some cases very much lower.

Waters of the temperate zone

Figs. 2 b1 and 2 b2 show vertical profiles of the quantum yield of photosynthesis for the temperate zone in summer. Fig. 2 b1 illustrates profiles for seas of dynamic-climatic types Case 1 (S–W) with a temperature of 20°C. As regards the tropical zone, there are five plots of $\Phi(z)$ corresponding to the trophic types O1, O2, O3, M, I. In comparison with the tropical regions, the maximum yield at the surface, $\Phi(0)$, in basins of trophic type I has fallen to around 0.011 mol C Ein^{-1}. Peak yields are roughly the same as in the tropical zone and occur at similar depths. There are few type 2 (M–W) basins with these same conditions; they are characterised by only one $\Phi(z)$ plot associated with trophic type I (see Fig. 2 b2).

The situation for temperate seas during winter is depicted in Figs. 2 b3 and 2 b4. The mean irradiance with respect to summer has fallen by 63% while the average temperature has dropped by 10°C. As a result of the lower winter temperatures, two additional eutrophic types of basins appear: on Fig. 2 b3 they are marked by the symbols E1 and E2. The maximum surface yield , $\Phi(0)$, rises to around 0.015 mol C Ein^{-1}, and the absolute $\Phi(z)$ maximum to c. 0.056 mol C Ein^{-1}. The other 'summer' profiles display a slight fall in yield in comparison with tropical waters in summer. The situation in Case 2 (M–W) waters, under the same conditions, is illustrated by the two plots associated with trophic types E1 and E2 (see Fig. 2 b4). For the same trophic types, therefore, the quantum yield of photosynthesis in temperate climatic zones is only slightly below that in tropical regions and has a distinct annual cycle.

The vertical profiles of primary production $P(z)$ for all the temperate zone waters indicated above are shown in Fig. 2, plots c1, c2, c3, c4. These plots show that in summer the absolute magnitudes of primary production at particular depths (and also the magnitudes of total production P_{tot} – see Table 2, middle part), as in the case of the yields $\Phi(z)$, are similar to the magnitudes of production for the same trophic types of tropical seas.

But unlike the case in the tropical zone, the temperate zone undergoes considerable seasonal variations in primary production. As a result of these changes, the absolute values of primary production recorded in winter are several times smaller.

Waters of the polar zone

Figs. 3 plots b1 and b2 show vertical profiles of the quantum yield of photosynthesis $\Phi(z)$ under polar conditions during summer. The former figure covers waters of the optical-dynamic-climatic type Case 1 (S–C) with a temperature of 5°C. The trophic types of waters to be found in this region are O1, O2, O3, M, I, E1, E2, E3. The surface yield $\Phi(0)$ in summer is significant only in eutrophic waters; elsewhere, its value is practically zero. The maximum yield $\Phi(z)$, e.g. for trophic type E3, is approximately 0.06 mol C Ein^{-1}. This value, which approaches the highest quantum yield of photosynthesis achieved under natural conditions in the sea, occurs at about the same depths as in the temperate zone. Waters of the dynamic-climatic type Case 2 (M–C) at the same temperature are described by two $\Phi(z)$ plots, which are associated with trophic types E2 and E3 (see Fig. 3 b2).

Figs. 3 b3 and 3 b4 show $\Phi(z)$ plots calculated for the polar zone in winter. By comparison with summer, the irradiance has fallen by 97%, and the temperature to 1°C. Because of this temperature drop, trophic type E3 does not occur in winter (see Fig. 3 b3). In all cases throughout the water column, the magnitudes of the yield $\Phi(z)$ are fairly high. The highest quantum yields are recorded in waters richest in chlorophyll. Under the same conditions, type Case 2 (M–C) waters are typified by the two $\Phi(z)$ plots associated with trophic types I and E1 (see Fig. 3 b4).

Fig. 3 plots c1, c2, c3, c4 present the vertical profiles of primary production for all the types of polar seas analysed above. They show that the absolute magnitudes of primary production at various depths, and also the absolute total production P_{tot} (see Table 2, lower part) are very much smaller than the corresponding magnitudes in waters of the same trophicity in the tropical and temperate zones. This is due mainly to the low insolation received by polar regions, especially in winter. This is why polar waters, especially oligotrophic ones, display a strong seasonality as regards the intensity of production. In winter, absolute magnitudes of production may drop to undetectable levels.

3. Validation of the multi-component model of primary production MCM as a satellite algorithm

Models linking primary production in the sea with the surface concentration of chlorophyll and auxiliary data such as the water temperature and

the PAR irradiance at or just below the sea surface permit the construction of algorithms for determining the magnitude of production on the basis of satellite data. This is the case of the MCM because the input parameters of this model can be estimated by remote sensing techniques.

In the final stage of the present work, we tested the MCM as a satellite algorithm for estimating primary production in stratified, mainly Case 1 Waters. To this end, 180 profiles of daily primary production in these waters were selected at random from the available data bank (a total of c. 1800 readings at various depths), for which the water temperature *temp*, the surface concentration of chlorophyll $C_a(0)$, and the daily PAR energy dose $\eta_{PAR}(0^+)$ just below the sea surface, among other factors, were known. These data were then used to compute primary productions at various depths in accordance with the algorithm given in Annex 1 of the MCM description (Woźniak et al. 2003). Instantaneous productions expressed in [atomC m^{-3} s^{-1}] are determined from the model directly. So in order to estimate the daily productions, as before (section 2), the sinusoidal variability of irradiance during the day was simulated appropriately and the daily sequence of changes in the instantaneous production determined. The next step was to integrate the instantaneous values over the duration of the day in order to obtain the daily total productions. Finally, the computed daily total productions were compared with *in situ* measurements with the traditional method with ^{14}C. This constituted the validation of the 'satellite' algorithm. The results are given in Fig. 4, and the calculated errors in the estimated production $P(z)$ at various depths are given in Table 3 (line A).

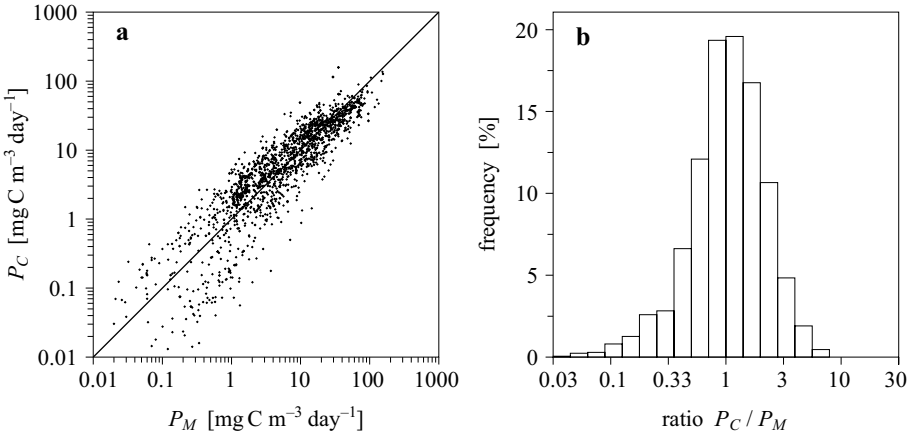

Fig. 4. Comparison of calculated P_C (with the MCM) and measured P_M primary production at various depths in the sea (a) and the histogram of P_C/P_M ratio (b)

Table 3. Relative errors of the determination of primary production at various depths in the sea calculated with the MCM:
A – with the quantum yield of photosynthesis as modelled in the MCM;
B – with the quantum yield of photosynthesis as given in Annex 1 (the previous model by Woźniak et al.);
C – with the quantum yield of photosynthesis as given in Annex 2 (the model by Morel et al.)

	Arithmetic statistics		Logarithmic statistics			
	systematic error $\langle\varepsilon\rangle$ [%]	statistical error σ_ε [%]	systematic error $\langle\varepsilon\rangle_g$ [%]	standard error factor x	statistical error σ_- [%]	σ_+ [%]
A	45.5	± 137	–3.34	2.142	–53.3	114
B	49.9	± 161	7.84	2.593	–61.4	159
C	65.4	± 164	26.5	2.441	–59.0	144

where

$\varepsilon = (P_c - P_M)/P_M$ – error,

$\langle\varepsilon\rangle$ – mean arithmetic error,

σ_ε – standard deviation (statistical error),

$\langle\varepsilon\rangle_g = 10^{[\langle\log(P_c/P_M)\rangle]} - 1$ – mean geometrical error,

$\langle\log(P_c/P_M)\rangle$ – mean $\log(P_c/P_M)$,

$x = 10^{\sigma_{\log}}$ – standard error factor,

$$\sigma_- = \frac{1}{x} - 1 \quad \text{and} \quad \sigma_+ = x - 1.$$

The results (line A in Table 3) indicate that the logarithmic systematic errors of the MCM algorithm are insignificant (e.g. $\langle\varepsilon\rangle_g \approx 3.3\%$). The logarithmic statistical errors, however, are greater (e.g. $\sigma_+ \approx 114\%$), particularly where production $P(z)$ is small (see Fig. 3a), that is, mostly at considerable depths. Nevertheless, at these same depths, traditional measurements of photosynthesis in the sea are also encumbered by colossal errors (Koblentz-Mishke et al. 1985). Moreover, the standard error factor $x = 2.14$ is relatively small in comparison with the range of variability of the estimated production, which covers some 4 orders of magnitude (from c. 0.01 to c. 100 and more mg C m^{-3} day^{-1}).

Over and above this, the tendency is that satellite techniques will be used with better accuracy to assess the global production P_{tot} in the water column beneath unit area. The next validation thus refers to these global productions P_{tot}.

The daily productions P_{tot} were determined by integrating numerically the vertical distributions of production, both measured and modelled with the MCM, over depth:

$$P_{\mathrm{tot}} = \int_0^{z_{\max}} P(z)dz,$$

where $z_{\max}$ was assumed to be 1.5 times the depth of the euphotic zone, i.e. $z_{\max} = 1.5z_e$ (below this depth photosynthesis production is insignificant and assumed to be zero).

The results of this validation are shown in line A of Table 4 and illustrated in Fig. 5. They show that the magnitudes of the errors in estimated total primary productions in the sea have fallen very substantially in comparison with the errors of estimating productions at different depths. The standard error factor of $x = 1.57$ here is relatively small and acceptable. To recapitulate: the test of the possible applications of the MCM as a satellite algorithm yielded positive results.

Table 4. Relative errors of the determination of total primary production in the water column, calculated with the MCM:
A – with the quantum yield of photosynthesis as modelled in the MCM;
B – with the quantum yield of photosynthesis as given in Annex 1 (the previous model by Woźniak et al.);
C – with the quantum yield of photosynthesis as given in Annex 2 (the model by Morel et al.)

	Arithmetic statistics		Logarithmic statistics			
	systematic error $\langle\varepsilon\rangle$ [%]	statistical error σ_ε [%]	systematic error $\langle\varepsilon\rangle_{\mathrm{g}}$ [%]	standard error factor x	statistical error σ_- [%]	σ_+ [%]
A	7.7	± 45.0	–2.68	1.569	–36.3	56.9
B	22.3	± 74.2	6.81	1.987	–49.7	99.7
C	41.8	± 68.1	20.5	1.862	–46.3	86.2

where

$\varepsilon = (P_{\mathrm{tot},C} - P_{\mathrm{tot},M})/P_{\mathrm{tot},M}$ – error,

$\langle\varepsilon\rangle$ – mean arithmetic error,

σ_ε – standard deviation (statistical error),

$\langle\varepsilon\rangle_{\mathrm{g}} = 10^{[\langle\log(P_{\mathrm{tot},C}/P_{\mathrm{tot},M})\rangle]} - 1$ – mean geometrical error,

$\langle\log(P_{\mathrm{tot},C}/P_{\mathrm{tot},M})\rangle$ – mean $\log(P_{\mathrm{tot},C}/P_{\mathrm{tot},M})$,

$x = 10^{\sigma_{\log}}$ – standard error factor,

$$\sigma_- = \frac{1}{x} - 1 \quad \text{and} \quad \sigma_+ = x - 1.$$

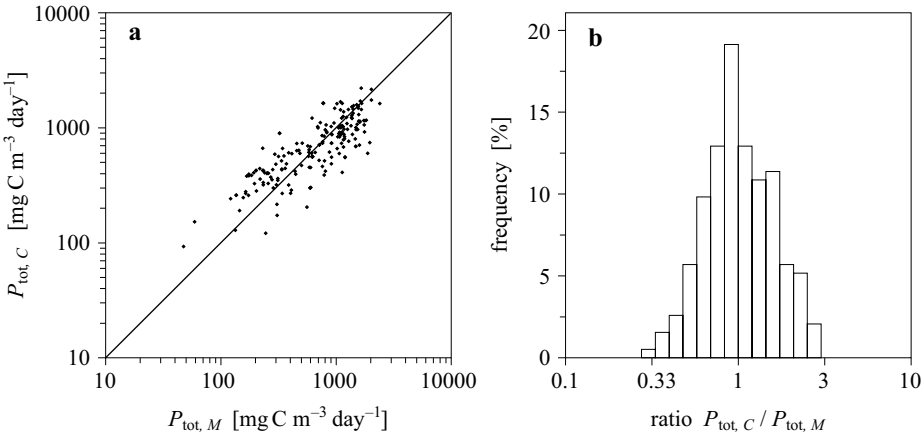

Fig. 5. Comparison of the total primary production in the water column of various ocean regions – measured $P_{\mathrm{tot},M}$ and calculated $P_{\mathrm{tot},C}$ with the MCM (a); and the histogram of $P_{\mathrm{tot},C}/P_{\mathrm{tot},M}$ ratio (b)

For comparison, primary production estimates were validated in like manner on the same empirical material using the earlier model expressions for the quantum yield of photosynthesis, i.e. the previous models by Woźniak et al. (Annex 1) and Morel et al. (Annex 2). To do this, the productions were also estimated on the basis of the algorithm given in Annex 1 of the MCM description, but with the additional use of the expression for the quantum yield of photosynthesis from Block 9 of the algorithm, appropriately altered (see Fig. 1 of the MCM description). Since in the Woźniak et al. and Morel et al. models the yield $\Phi(z)$ does not depend on the nutrient concentration, blocks 8 and 14 of the MCM (Fig. 1 in the MCM description) were not invoked in these calculations, and the yields $\Phi(z)$ were determined solely from the relevant concentrations of chlorophyll a and the water temperature. The computed errors of the productions estimated with the aid of these models in both cases, that is, for productions at given depths in the sea $P(z)$ and the total production in the water column P_{tot}, are included in the tables of errors (Table 3 and Table 4 – lines B and C). The ranges of these errors are greater by several tens of percentage points than those encumbering primary productions estimated using the new MCM. This vindicates our efforts to modify the model description of the quantum yield of marine photosynthesis in such a way that the direct influence of nutrients (in this case N_{inorg}) on the photosynthesis process is taken into account.

4. Summary and conclusions

The present article brings to a close another stage in the development of a state-of-the-art, innovative model of marine photosynthesis, particularly in Case 1 Waters, which our team of scientists at Sopot has been working on in recent years.

During the modelling process we have developed detailed semi-empirical models of most of the light-stimulated processes occurring in marine algae in different trophic types of sea, for example, photo-acclimation and the production of photoprotecting carotenoids (see e.g. Woźniak et al. 1997, Majchrowski & Ostrowska 1999), chromatic acclimation and the production of various forms of chlorophyll-antennas and photosynthetic carotenoids (Majchrowski & Ostrowska 2000, Majchrowski 2001), adaptation of cells by the package effect (Woźniak et al. 1999), light absorption (Majchrowski et al. 2000, Woźniak et al. 2000), photosynthesis of organic matter and the quantum yield of this process (Ficek 2001, Woźniak et al. 2002a), photoinhibition (Ficek 2001), the fluorescence effect (Ostrowska et al. 2000a, b, Ostrowska 2001) and the activation of PS2 centres (see Ficek et al. 2000a).

The multi-component marine photosynthesis model (MCM) has been developed by a synthesis of these detailed models applicable to the principal photophysiological processes occurring in algae, as well as a few other models describing the spatial distributions of chlorophyll and the irradiance transmittance in the sea (e.g. Woźniak et al. 1992a, b, 1997a, b, Kaczmarek & Woźniak 1995). The MCM is discussed in detail in a number of articles, e.g. the one by Woźniak et al. (2003). This model is by nature a physical one, in which the constants have been determined on the basis of statistical analyses of empirical material. The key relationship in this model is the one between the quantum yield of photosynthesis at various depths in the sea and such environmental factors as the irradiance conditions, concentration of nitrogenous nutrients and temperature in the sea, and also the sea's trophicity, the quantitative index of which is the surface concentration of chlorophyll *a*. This latter factor enables such yields to be determined, and also a variety of photosynthetic characteristics of the sea, notably the primary production, on the basis of the above-mentioned data.

A further practical advantage of the MCM is that the set of model relationships also includes a series of statistical regularities referring to the interdependences between chlorophyll *a* concentrations, nitrogenous nutrient contents and the temperature in the sea, all described by approximate mathematical formulas. Hence, vertical distributions of nitrogenous nutrients can be estimated from known surface concentrations of chlorophyll *a* and temperatures in the sea. This is an essential aspect of the 'satellite'

algorithm for determining the photosynthetic characteristics of the sea, which provides for the direct estimation of distributions of nitrogenous nutrients. Moreover, it enables the quantum yield of photosynthesis and primary production at any depth in the sea to be estimated indirectly on the basis of three input data: the surface concentration of chlorophyll a, the solar irradiance at the sea surface and the surface temperature of the sea water. Since these data are obtainable by *remote sensing* methods, the MCM satisfies the conditions of a 'satellite' model.

The present article, which concludes the stage of work devoted to finding a state-of-the-art model of marine photosynthesis, demonstrates the practical utility of the MCM:

- The MCM has been applied successfully to the analysis of the natural variability in the quantum yields of photosynthesis characteristic of different trophic types of sea in different geographical regions at different seasons and different depths in the sea. This analysis is presented in detail in section 2. The results have shown up a number of regularities in the spatial and temporal differentiation of photosynthetic characteristics and the primary production of phytoplankton in the World Ocean. While they are generally well-known from empirical studies, they are restated here in more systematic and quantitatively more precise terms.

- The MCM has been tested and empirically validated from the standpoint of its possible application in the satellite scanning of primary production in Case 1 Waters. To this end, the relevant *in situ* measured values of this production were compared with the corresponding values obtained from the model on the basis of input data from *remote sensing*. For comparison, similar validations were done in which the latest expression for the quantum yield of photosynthesis in the MCM was replaced with the appropriate expressions from the earlier models by Woźniak et al. (Annex 1) and Morel et al. (Annex 2). The results of the validation have vindicated the utility of the MCM in satellite scanning algorithms for primary production and demonstrated its superiority over the earlier models. To take just one example: the statistical errors of the estimate σ_ε of the overall primary production in the water column (Table 4) are $\pm$ 45% for the MCM, but as high as 68% for the earlier model by Morel et al. and 74% for the earlier model by Woźniak et al.

5. Final remarks

The modelling of marine photosynthesis which we have presented in our papers applies largely to oceanic basins with Case 1 Waters. Its applicability to Case 2 Waters is limited and the results are not satisfactory. All processes involving light, and so also photosynthetic primary production, are strongly influenced in such waters by a whole range of allogenic, optically active substances derived from rivers, the atmosphere, sea beds and sea shores.

Another drawback of our model is the fact that at the present stage it is based on the assumption that nitrogen is the nutrient limiting photosynthesis. We are well aware that in many areas of the World Ocean, both in Case 2 and in Case 1 waters, at certain seasons primary production may be limited by other nutrients.

To enable our model to take account of these drawbacks is the objective of our future studies; it will be based on the analysis of numerous new sets of empirical data which are currently being gathered – as part of the research project PBZ–KBN 056/P04/2001 'The investigation and development of a satellite system for monitoring the Baltic ecosystem' – from Baltic basins classified as Case 2 Waters, and also from other shelf and enclosed seas.

References

Antoine D., Morel A., 1996, *Oceanic primary production: 1. Adaptation of spectral light-photosynthesis model in view of application to satellite chlorophyll observations*, Global Biogeochem. Cycles, 10 (1), 42–55.

Dera J., 1995, *Underwater irradiance as a factor affecting primary production*, Diss. and monogr., Inst. Oceanol. PAS, Sopot, 7, 110 pp.

Ficek D., 2001, *Modelling the quantum yield of photosynthesis in different marine basins*, Rozpr. i monogr., Inst. Oceanol. PAN, Sopot, 14, 224 pp., (in Polish).

Ficek D., Ostrowska M., Kuzio M., Pogosyan S. I., 2000a, *Variability of the portion of functional PS2 reaction centres in the light of a fluorometric study*, Oceanologia, 42 (2), 243–249.

Ficek D., Woźniak B., Majchrowski R., Ostrowska M., 2000b, *Influence of non-photosynthetic pigments on the measured quantum yield of photosynthesis*, Oceanologia, 42 (2), 231–242.

Gershanovich D. E., Muromtsev A. M., 1982, *Oceanological principles of the biological productivity of the world ocean*, Gidrometeoizdat, Leningrad, 320 pp., (in Russian).

Kaczmarek S., Woźniak B., 1995, *The application of the optical classification of waters in the Baltic Sea (Case 2 Waters)*, Oceanologia, 37 (2), 285–297.

Koblentz-Mishke O. I., Woźniak B., Ochakovskiy Yu. E. (eds.), 1985, *Utilisation of solar energy in the photosynthesis of the Baltic and Black Sea phytoplankton*, Inst. Okeanol. AN SSSR, Moskva, 336 pp., (in Russian).

Majchrowski R., 2001, *Influence of irradiance on the light absorption characteristics of marine phytoplankton*, Stud. i rozpr., Pom. Akad. Pedag., Słupsk, 1, 131 pp., (in Polish).

Majchrowski R., Ostrowska M., 1999, *Modified relationships between the occurrence of photoprotecting carotenoids of phytoplankton and Potentially Destructive Radiation in the sea*, Oceanologia, 41 (4), 589–599.

Majchrowski R., Ostrowska M., 2000, *Influence of photo- and chromatic acclimation on pigment composition in the sea*, Oceanologia, 42 (2), 157–175.

Majchrowski R., Woźniak B., Dera J., Ficek D., Kaczmarek S., Ostrowska M., Koblentz-Mishke O. I., 2000, *Model of the 'in vivo' spectral absorption of algal pigments. Part 2. Practical applications of the model*, Oceanologia, 42 (2), 191–202.

Morel A., 1991, *Light and marine photosynthesis: a spectral model with geochemical and climatological implications*, Prog. Oceanogr., 26, 263–306.

Morel A., Antoine D., Babin M., Dandonneau Y., 1996, *Measured and modeled primary production in the northeast Atlantic (Eumeli JGOFS program): the impact of natural variations in photosynthetic parameters on model predictive skill*, Deep-Sea Res., 43, 1273–1304.

Morel A., Prieur L., 1977, *Analysis of variations in ocean color*, Limnol. Oceanogr., 22 (4), 709–722.

Ostrowska M., 2001, *Using the fluorometric method for marine photosynthesis investigations in the Baltic*, Rozpr. i monogr., Inst. Oceanol. PAN, Sopot, 15, 194 pp., (in Polish).

Ostrowska M., Majchrowski R., Matorin D. N., Woźniak B., 2000a, *Variability of the specific fluorescence of chlorophyll in the ocean. Part 1. Theory of classical 'in situ' chlorophyll fluorometry*, Oceanologia, 42 (2), 203–219.

Ostrowska M., Matorin D. N., Ficek D., 2000b, *Variability of the specific fluorescence of chlorophyll in the ocean. Part 2. Fluorometric method of chlorophylla determination*, Oceanologia, 42 (2), 221–229.

Timofeyev N. A., 1983, *Radiation regime of the ocean*, Nauk. Dumka, Kiyev, 247 pp., (in Russian).

Woźniak B., Dera J., 2000, *Luminescence and photosynthesis of marine phytoplankton – a brief presentation of new results*, Oceanologia, 42 (2), 137–156.

Woźniak B., Dera J., 2001, *Bio-optical modelling of the photo-physiological properties of marine algae*, pp. 39–49, Proc. St. Petersburg Int. Conf. 'Current problems in optics of natural waters' (ONW–2001), September 25–28, 2001.

Woźniak B., Dera J., Ficek D., Majchrowski R., Kaczmarek S., Ostrowska M., Koblentz-Mishke O. I., 1999, *Modelling the influence of acclimation on the absorption properties of marine phytoplankton*, Oceanologia, 41 (2), 187–210.

Woźniak B., Dera J., Ficek D., Majchrowski R., Kaczmarek S., Ostrowska M., Koblentz-Mishke O. I., 2000, *Model of the 'in vivo' spectral absorption of algal pigments. Part 1. Mathematical apparatus*, Oceanologia, 42 (2), 177–190.

Woźniak B., Dera J., Ficek D., Majchrowski R., Ostrowska M., Kaczmarek S., 2003, *Modelling light and photosynthesis in the marine environment*, Oceanologia, 45 (2), 171–245.

Woźniak B., Dera J., Ficek D., Ostrowska M., Majchrowski R., 2002a, *Dependence of the photosynthesis quantum yield in oceans on environmental factors*, Oceanologia, 44 (4), 439–459.

Woźniak B., Dera J., Ficek D., Ostrowska M., Majchrowski R., Kaczmarek S., Kuzio M., 2002b, *The current bio-optical study of marine phytoplankton*, Opt. Appl., 32 (4), 731–747.

Woźniak B., Dera J., Koblentz-Mishke O. I., 1992a, *Bio-optical relationships for estimating primary production in the Ocean*, Oceanologia, 33, 5–38.

Woźniak B., Dera J., Koblentz-Mishke O. I., 1992b, *Modelling the relationship between primary production, optical properties, and nutrients in the sea*, Ocean Optics 11, Proc. SPIE, 1750, 246–275.

Woźniak B., Dera J., Majchrowski R., Ficek D., Koblentz-Mishke O. I., Darecki M., 1997, *'IO PAS initial model' of marine primary production for remote sensing application*, Oceanologia, 39 (4), 377–395.

Woźniak B., Dera J., Semovski S., Hapter R., Ostrowska M., Kaczmarek S., 1995a, *Algorithm for estimating primary production in the Baltic by remote sensing*, Stud. i Mater. Oceanol., 68, 91–123.

Woźniak B., Smekot-Wensierski W., Darecki M., 1995b, *Semi-empirical modelling of backscattering and light reflection coefficients in WC1 seas*, Stud. i Mater. Oceanol., 68, 61–90.

Annex 1

The previous model of the photosynthesis quantum yield according to Woźniak et al.

The model developed by Woźniak and his co-workers enabled quantum yields of photosynthesis to be estimated at various depths in the sea $\Phi(z)$ on the basis of environmental factors, such as the irradiance PAR, the temperature *temp*, and the surface concentration of chlorophyll $C_a(0)$, which was taken to be the index of trophicity of the sea. The model constants were determined on the basis of the statistical analysis of sets of appropriate empirical data gathered by the Institute of Oceanology PAS in Sopot, the Institute of Oceanology RAS in Moscow, and the Department of Biophysics of the Lomonosov University in Moscow. This model was constructed in stages (see Woźniak et al. 1992a, b, Woźniak 1995b). Initially, it was assumed that the quantum yield of photosynthesis could be written as the product of the maximum yield and the light factor f_E:

$$\Phi = \Phi_{\max}\ f_E, \tag{A1-1}$$

where

$\Phi_{\max}$ – the maximum quantum yield of photosynthesis, which is the yield recorded at low irradiances ($PAR \to 0$); the other factors governing photosynthesis remain constant;

f_E – the light factor describing the fall in the photosynthetic yield in the presence of non-zero natural irradiance.

The maximum yield of photosynthesis at any depth in the sea became associated with the trophic type of the basin, the index of which is the surface concentration of chlorophyll a, $C_a(0)$. This relationship took the form:

$$\Phi_{\max} = 0.051\ \frac{C_a(0)^{0.66}}{0.44 + C_a(0)^{0.66}}\quad [\text{mol C Ein}^{-1}]. \tag{A1-2}$$

The influence of irradiance was taken into account by the use of a hyperbolic Michaelis–Menten function of the form:

$$f_E(z) = \frac{PAR_{1/2}}{PAR_{1/2} + PAR(z)}, \tag{A1-3}$$

where

$PAR_{1/2}$ – irradiance in the spectral range PAR, where the real quantum yield $\Phi = \frac{1}{2}\Phi_{\max}$.

An expression for the quantum yield of photosynthesis taking other abiotic factors into consideration, i.e. temperature and inhibition, was given later in Dera, 1995. The relation between Φ and temperature was introduced

into the expression for $PAR_{1/2}$ (in eq. (A1-3)) in the form of Arrhenius' Law:

$$PAR_{1/2}(temp) = 5.25 \times 10^{-5} \times 2^{temp[^\circ\mathrm{C}]/10} \quad [\mathrm{Ein\ m^{-2}\ s^{-1}}]. \tag{A1-4}$$

The final expression for the light factor described by equation (A1-3) is as follows:

$$f_{E,t}(temp,\, z) = \frac{PAR_{1/2}(temp)}{PAR_{1/2}(temp) + PAR(z)}. \tag{A1-5}$$

A second parameter *temp* has appeared as a result of introducing temperature into the equation. On the other hand, the factor describing photoinhibition was expressed by the relation:

$$I(PAR) = e^{-\beta\ PAR}, \tag{A1-6}$$

where

$$\beta = 2.95 \times 10^3\ \mathrm{m^2\ s\ Ein^{-1}}.$$

The complete expression for the yield Φ can therefore be given in the form:

$$\left.\begin{aligned} \Phi[C_a(0),\, PAR,\, temp] = 0.051\ \times\ & \frac{C_a(0)^{0.66}}{0.44 + C_a(0)^{0.66}}\ \times \\ & \times \frac{PAR_{1/2}(temp)}{PAR_{1/2}(temp) + PAR(z)}\ \times e^{-\beta\ PAR} \\ & [\mathrm{mol\,C\ Ein^{-1}}] \\ \beta = 2.95 \times 10^3 \quad & [\mathrm{m^2\ s\ Ein^{-1}}] \\ PAR_{1/2} = 5.25 \times 10^{-5} \times 2^{temp[^\circ\mathrm{C}]/10} \quad & [\mathrm{Ein\ m^{-2}\ s^{-1}}] \end{aligned}\right\}. \tag{A1-7}$$

This form of the expression for Φ was used in the present paper for the comparative assessment of the errors of estimation.

Annex 2

The model of the photosynthesis quantum yield according to Morel et al.

The model of the quantum yield of photosynthesis developed by the French team of A. Morel was described in the following papers: Morel (1991), Antoine & Morel (1996), Morel et al. (1996). Like the Woźniak model (discussed in Annex 1), Morel's model described the relation between the quantum yield of photosynthesis Φ and the principal environmental factors, i.e. irradiance, chlorophyll concentration and temperature. The main formula of this model is also the product of the maximum yield $\Phi_{\max}$ and the light factor $f_{E,t}$, which at the same time takes the effect of temperature into account:

$$\Phi = \Phi_{\max} \; f_{E,t}, \tag{A2-1}$$

where

$\Phi_{\max}$ – maximum yield of photosynthesis under given environmental conditions (i.e. for low irradiances $PAR \approx 0$);

$f_{E,t}$ – the light factor describing the relation between the yield of photosynthesis and the irradiance, dependent on the level of this irradiance and additionally on the temperature *temp* (hence the second subscript 't' in the symbol for the factor $f_{E,t}$).

In this model the maximum yield depends on the real concentration of chlorophyll a at a given depth $C_a(z)$, and not on the trophic index of the basin $C_a(0)$ as in Woźniak's model (Annex 1). This equation takes the form:

$$\Phi_{\max}(z) = 0.034 \; [C_a(z)]^{0.33} \quad [\text{mol C Ein}^{-1}]. \tag{A2-2}$$

The expression for the light factor includes the energy absorbed by phytoplankton cells PUR^* and the temperature *temp*:

$$f_{E,t}(temp,\, z) = x^{-1} \; (1 - e^{-x}) \; e^{-\beta x}, \tag{A2-3}$$

where $\beta = 0.01$ [dimensionless];

$$x = \frac{PUR^*(z)}{KPUR^*(temp,\, z)};$$

$$KPUR^*(temp,\, z) = [C_a(z)]^{-0.33} \times 32.2 \times 10^{-7} \times (1.88)^{\frac{temp - 20^\circ\text{C}}{10}}$$

$$[\text{Ein (mg tot. chl } a)^{-1}\ \text{s}^{-1}]$$

$$PUR^*(z) \cong \frac{1.2}{C_a(z)} \int_{400\,\text{nm}}^{700\,\text{nm}} E_d(\lambda,\, z) \; a_{pl}(\lambda,\, z) d\lambda$$

(energy absorbed by phytoplankton per unit mass of chlorophyll a).

The complete expression for the yield thus takes the form:

$$\left.\begin{aligned} \Phi[C_a,\, PUR^*,\, temp] &= 0.034\ C_a^{0.33}\ x^{-1} \times \\ &\quad \times (1 - e^{-x})\ e^{-\beta x} \quad [\mathrm{mol\,C\ Ein^{-1}}] \\ \beta &= 0.01 \\ x &= \frac{PUR^*}{C_a^{-0.33}\ 32.2 \times 10^{-7} \times (1.88)^{\frac{temp - 20^\circ\,\mathrm{C}}{10}}} \end{aligned}\right\}. \tag{A2-4}$$

It is this form of the expression for Φ that was used in the comparative assessment of the estimation errors in this article.

Annex 3

List of symbols and abbreviations denoting the physical quantities used in this paper and division of marine basins into biological types:

Symbol	Denotes	Units
a_{pl}	light absorption coefficient of phytoplankton	m^{-1}
C_a	sum of chlorophylls a + pheo, or total chlorophyll (chl a + divinyl chl a) concentrations	mg tot. chl a m^{-3}
$C_a(0)$ $C_a(z)$	sum of chlorophylls a + pheo, or total chlorophyll (chl a + divinyl chl a) concentrations in the surface water, at depth z	mg tot. chl a m^{-3}
$E_d(\lambda)$	spectral downward irradiance	Ein m^{-2} s^{-1} nm^{-1}
f_E	the light factor describing the fall in the photosynthesis yield in the presence of non-zero natural irradiance	dimensionless
$f_{E,t}$	the classical dependence of photosynthesis on light and temperature	dimensionless
$KPUR^*$	photosynthesis saturation PUR energy	Ein (mg tot. chl a)$^{-1}$ s^{-1}
N_{inorg}	concentration of inorganic nitrogen	μM
P	primary production in the sea	mg C m^{-3} day^{-1}
P_{tot}	total primary production in water column	gC m^{-2} day^{-1}
PAR	photosynthetically available radiation	
PAR	irradiance of photosynthetically available radiation	Ein m^{-2} s^{-1}
$PAR_{1/2}$	irradiance in the spectral PAR range, where the real quantum yield equals half of maximum value	Ein m^{-2} s^{-1}
PUR^*	photosynthetically utilised radiation (per unit of chlorophyll a mass)	Ein (mg tot. chl a)$^{-1}$ s^{-1}

Annex 3

List of symbols and abbreviations (*continued*)

Symbol	Denotes	Units
Trophic type symbols:		
O	oligotrophic	
M	mesotrophic	
I	intermediate	
E	eutrophic	
$temp$	temperature in the euphotic zone	°C
t_d	duration of daylight	h
z	depth in the sea	m
z_e	depth of the euphotic zone (level of 1% of the surface PAR irradiance)	m
z_m	mixing depth	m
$\Phi_{\max}$	maximum quantum yield of carbon fixation	mol C Ein^{-1}
Φ_1	observed quantum yield of carbon fixation	mol C Ein^{-1}
Φ_2	true quantum yield of carbon fixation	mol C Ein^{-1}
λ	light wavelength	nm
$\eta_{PAR}(0^+)$	the daily radiation dose of the PAR spectrum range	Ein m^{-3} day^{-1}
$<\eta_{\text{day}}>_{\text{month}}$	monthly mean total daily doses of solar irradiance at the sea surface	MJ m^{-2} day^{-1}
(0^+)	level just below the sea surface	m

Table A3.1. Division of marine basins into biological types

Trophic type	Symbol	Range of C_a concentration [mg m^{-3}]	Mean C_a concentration [mg m^{-3}]
oligotrophic	O1	0.02–0.05	0.035
	O2	0.05–0.10	0.075
	O3	0.10–0.20	0.15
mesotrophic	M	0.2–0.5	0.35
intermediate	I	0.5–1.0	0.75
eutrophic	E1	1–2	1.5
	E2	2–5	3.5
	E3	5–10	7.5
	E4	10–20	15
	E5	> 20	–